Clays and Clay Minerals, Vol. 61, No. 3, 193–203, 2013.

SYNTHESIS, CHARACTERIZATION, AND EVALUATION OF A FERROMAGNETICALLY MODIFIED NATURAL ZEOLITE COMPOSITE FOR REMOVAL OF Cs^+ AND Sr^{2+}

HOSSEIN FAGHIHIAN[1,*], MOHAMMAD MOAYED[1], ALIREZA FIROOZ[1], AND MOZHGAN IRAVANI[1,2]

[1] Department of Chemistry, University of Isfahan, 81746-73441, Isfahan, Iran
[2] Nuclear Fuel Cycle Research School, Nuclear Science and Technology Research Institute, Isfahan, Iran

Abstract—The high fission yield and long half life of cesium and strontium make them the two most high-risk products from nuclear fission, so their separation from radioactive wastes is an important step in mitigating their harmful effects. Clinoptilolite, because of its thermal stability, high radiation resistance, and selectivity, was considered as the adsorbent for this purpose. In order to then separate the adsorbent-adsorbate complex from aqueous solution, the clinoptilolite was prepared as a magnetized composite with nanomagnetite. This magnetically modified zeolite enabled the efficient and quick separation of the adsorbent from solution using magnetic separation. The ability of this composite to remove Cs^+ and Sr^{2+} from aqueous solutions was assessed and characterized using X-ray diffraction, X-ray fluorescence, Fourier-transform infrared spectroscopy, differential thermogravimetric analysis, and vibrating-sample magnetometry. Variables such as initial ion concentration, pH, contact time, and temperature in the sorption process were studied and optimized. The maximum adsorption capacities of the composite were 188.7 and 36.63 mg g^{-1} for Cs^+ and Sr^{2+}, respectively. Investigation of the kinetics revealed that the adsorption process onto the composite was quicker than in the case of the zeolite alone. The equilibrium data were analyzed using the Langmuir, Freundlich, and Dubinin-Radushkevich (D-R) isotherm models. The mean free energy of sorption (E) for both ions was in the range 8−16 kJ mol^{-1}, confirming that an ion-exchange mechanism had occurred. Positive ΔH^o and negative ΔG^o values were indicative of the endothermic and spontaneous nature of the removal of Cs^+ and Sr^{2+}. The saturation magnetization of the composite was measured (17.46 Am^2/kg), implying fast magnetic separation of the sample after adsorption. The results obtained revealed that the natural Iranian zeolite nanomagnetite composite was a good ion exchanger in the removal of Cs^+ and Sr^{2+}.

Key Words—Cesium, Clinoptilolite, Composite, Nanomagnetite, Natural Zeolite, Strontium.

INTRODUCTION

Radioactive wastes containing radionuclides are considered to be the most hazardous environmental pollutants and their treatment has received much attention. Because of their high fission yields and long half-life properties, ^{137}Cs and ^{90}Sr are the two most notable fission products. Ion exchange, precipitation, liquid-liquid extraction, and adsorption are the traditional methods used for removal of cesium and strontium from liquid wastes, with ion exchange being the most effective technique (Balarama Krishna *et al.*, 2004; Shakir *et al.*, 2007; Wu *et al.*, 2012; Zhang *et al.*, 2009).

Zeolites, as inorganic ion exchangers with high thermal, mechanical, and radiation stability, and with good selectivity and exchange-capacity properties, are generally preferred over other adsorbents for removal of radionuclides from aqueous solution (Abdel Rahman *et al.*, 2010; Borai *et al.*, 2009; El-Naggar *et al.*, 2008). Radioactive wastes have been treated using natural zeolites such as mordenite, erionite, chabazite, and clinoptilolite. The last one is the most abundant natural zeolite with large selectivity and adsorption capacity (Kabiri-Tadi and Faghihian, 2011).

In clinoptilolite, AlO_4 and SiO_4 tetrahedra are linked together by sharing their oxygen atoms in the zeolite framework. In the substitution of Al(III) for Si(IV) in the structure of zeolites, a negative charge appears which is neutralized by exchangeable cations such as Na^+, K^+, Ca^{2+}, and Mg^{2+}. The selectivity and ion-exchange ability depend greatly on the numbers, types, and locations of these exchangeable cations in the zeolite framework, which may vary from one deposit to another and even within the same deposit. The clinoptilolite selected for the present study was obtained from the Aftar deposit located northwest of Semnan in northeast Iran.

After the ion-exchange process, one of the greatest challenges with zeolite powders is their separation from solution, a time-consuming and laborious procedure. This problem could be overcome by using a magnetic-separation technique. Magnetic modification offers a new methodology with efficient, precise, and quick separation of zeolite to which a magnetic field is applied. Magnetic composites have been used for the removal and preconcentration of ions from aqueous solution. Ashtari *et al.* (2005) used neocuproine-

* E-mail address of corresponding author:
h.faghih@sci.ui.ac.ir
DOI: 10.1346/CCMN.2013.0610303

modified magnetic microparticles for separation of Cu^{2+}. Bachir *et al.* (2009) studied the properties of magnetic Ti-pillared clay minerals. Gutierrez *et al.* (2010) prepared a magnetic composite by wet impregnating a powder of natural zeolite with a magnetic Fe oxide-containing synthetic material. Nah *et al.* (2006) prepared a composite of clinoptilolite, magnetite, and urethane for removal of Pb^{2+}. Oliveira *et al.* (2004) prepared a magnetic zeolite-Y composite for removal of Cr^{3+}, Cu^{2+}, and Zn^{2+}. Bourlinos *et al.* (2003) decorated the external surface of zeolite-Y with maghemite, and used it for adsorption of Hg^{2+}.

In the present study, the adsorption feature of natural clinoptilolite with magnetic properties of iron oxide was combined to prepare a nanomagnetite zeolite composite. The composite prepared was used to remove Cs^{+} and Sr^{2+} from aqueous solution and subsequently was separated from solution by simple magnetic separation. Different variables such as contact time, temperature, pH, and initial ion concentrations were investigated and optimized. The kinetics, thermodynamic, and isotherm parameters of the process were also evaluated.

EXPERIMENTAL

Materials and reagent

All chemical reagents used in this study were of analytical reagent grade (AR Grade). $FeCl_3{\cdot}6H_2O$ (Sigma-Aldrich, Germany, 98%) and $FeCl_2{\cdot}4H_2O$ (Sigma-Aldrich, Germany, 99%) were used for magnetic particle preparation. Cesium and strontium were supplied as cesium chloride and strontium chloride by Merck, Germany. Natural clinoptilolite was collected from the Aftar deposit located northwest of Semnan, Iran. In order to remove soluble salts, the zeolite was dispersed in distilled water and stirred for 12 h at 343 K in a round-bottom flask under reflux conditions. The purified zeolite was separated by centrifugation, dried at 110ºC in air, crushed and pulverized in a mortar, and the particle size between 200 and 400 μm collected by dry sieving. The powder was stored in a desiccator over saturated NaCl solution in order to maintain constant water content throughout the experiments.

Synthesis of the nanomagnetite zeolite composite

The magnetic zeolite composite (MZC) was prepared through co-precipitation of Fe^{3+} and Fe^{2+} in the presence of zeolite powder. Aqueous ammonia solution (100 mL of 1 M NH_4OH) was placed in a round-bottom flask with three access ports (one for N_2 gas, one for $FeCl_3$ and $FeCl_2$ solution, and one for the stirrer shaft) to which 3.5 g of zeolite powder was added. The mixture was stirred vigorously using a mechanical stirrer and deoxygenated by bubbling N_2 gas (99.99%) for 30 min. Solutions of ferric chloride (1 M $FeCl_3$ in water) and ferrous chloride (2 M $FeCl_2$ in 2 M HCl) with a volume ratio of 4:1 were prepared and mixed together. The Fe^{3+}/Fe^{2+} solution was added drop-wise to the zeolite/ammonia mixture while the mixture was stirred vigorously under N_2 atmosphere. The resulting composite was then separated from solution with the aid of a permanent magnet. Finally, the separated product was washed four times with deionized-deoxygenated water and then dried at 50ºC for 5 h (the product was protected from exposure to the atmosphere by applying a magnetic field under nitrogen atmosphere).

Characterization of the samples

The structural phase identification of samples was examined using a Bruker (Germany) D8 ADVANCE X-ray diffractometer (XRD). The chemical composition of the samples was determined using a PANalytical (The Netherlands) Magix X-ray fluorescence (XRF) spectrometer. The Fourier-transform infrared (FTIR) spectra were obtained using a Shimadzu (Japan) IR Prestige-21 Model spectrophotometer. Thermal analysis was performed using a Mettler (USA) TG-50 thermal analyzer with a heating rate of 10ºC min^{-1}. A vibrating-sample magnetometer (Meghnatis Daghigh Kavir Co., Kashan, Iran) was used to characterize the magnetic properties of the composite (the magnetic field applied was between 0 and 10,000 Oe). The concentration of cesium and strontium ions was determined using an inductively coupled plasma-atomic emission spectroscopy (ICP-AES) technique (GBC integra XL, Australia).

The cation exchange capacity (CEC) of the natural zeolite and the magnetic composites was determined by shaking 1.0 g of the samples with 100 mL of 1 M NH_4NO_3 solution at 25ºC for 72 h. The ammonium concentration was determined by the Kjeldahl method (Archibald and Seligson, 1957). Theoretical cation exchange capacity (TCEC) was calculated from chemical composition of the samples as a sum of exchangeable cations present in 1.0 g of zeolite.

Metal ion-uptake experiments

Adsorption experiments were carried out by stirring 0.2 g of zeolite sample or magnetic composite with 20 mL of 0.01 N Cs^{+} and Sr^{2+} solution at 298 K in a controlled-temperature rotary shaker (Pars Azma Co., Isfahan, Iran). After equilibration, the zeolite samples were separated by centrifugation while the composite was separated using a permanent magnet. The effect of pH on the sorption process was studied by adjusting the initial pH at 3−8 using 0.1 N HNO_3 and 0.1 N NaOH solutions. To study the kinetics, the samples were placed in contact with ion solutions for different periods of time (between 2 and 48 h). All experiments were conducted with 0.01 N ion solutions at 298 K except for temperature-dependence studies where the temperature varied between 298 and 343 K. The ion-exchange isotherms were constructed from the data obtained at different initial concentrations for Cs^{+} and Sr^{2+} (0.001−0.1 N).

https://doi.org/10.1346/CCMN.2013.0610303 Published online by Cambridge University Press

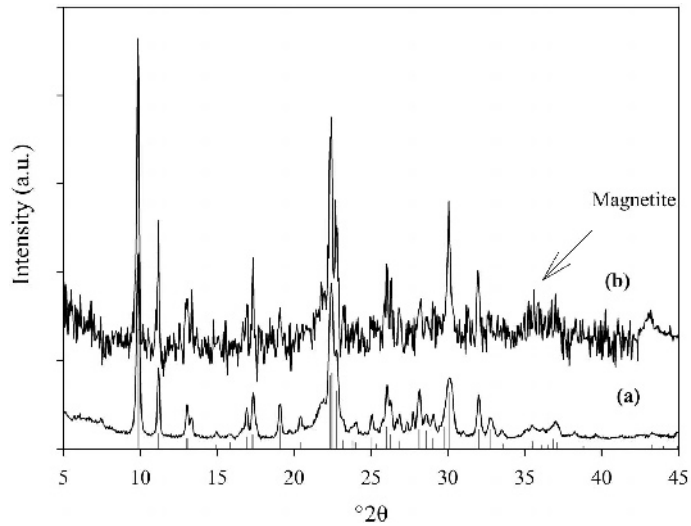

Figure 1. XRD patterns of the natural zeolite (matched with reference pattern of clinoptilolite) (a) and MZC (b).

The amount of ions adsorbed per unit mass of the adsorbent, q (meq g^{-1}), was calculated as:

$$q = (C_i - C_f) \times V/m \quad (1)$$

The distribution coefficient k_d (mL g^{-1}) was also calculated as:

$$k_d = (C_i - C_f)/C_f \times (V/m) \quad (2)$$

where C_i and C_f were the initial and final concentrations (meq mL^{-1}), respectively; m was the amount of the adsorbent (g), and V was the volume of the solution (L).

RESULTS AND DISCUSSION

Characterization of the adsorbents

The XRD patterns of the MZC and natural zeolite (Figure 1) correspond with reference patterns of clinoptilolite (Treacy and Higgins, 2007) demonstrating that clinoptilolite was the prevalent phase in the zeolite-rich rock. The line positions and relative intensities of the composite remained intact, showing that the crystal structure of zeolite was not changed during preparation of the composite. The XRD diffraction line at 35.55°2θ of the composite (Figure 1) corresponded to magnetite (Maity and Agrawal, 2007). Using Scherrer's equation (Klug and Alexander, 1974), the particle size of the nanomagnetite was found to be 24.7 nm

The chemical composition of the composite and natural zeolite (Table1) was obtained using XRF. The composite consisted of 19.86 wt.% Fe_2O_3. The Si/Al ratio of the present zeolite sample was 4.85, which is consistent with previous findings placing the ratio within the range of 4–5.5 (Breck, 1974). The theoretical cation exchange capacity (TCEC) was estimated as the sum of exchangeable ions, including Na^+, K^+, Ca^{2+}, and Mg^{2+}, in the zeolite. The difference between TCEC and CEC (Table 1) was ascribed to the fact that some of the counter-ion sites in the zeolite particles were unavailable for cation exchange.

The FTIR spectrum of the natural zeolite and MZC were recorded over the range 400–4000 cm^{-1} (Figure 2). Zeolites are significantly hydrated materials, and water absorption bands at 1636 cm^{-1} and in the range 3000–3600 cm^{-1} confirmed it. The band at 1070 cm^{-1} was assigned to asymmetric stretching vibration modes of internal T–O bonds in TO_4 tetrahedra (T = Si and Al). The bands at 794 and 465 cm^{-1} arise from the stretching vibration modes of O–T–O groups and the bending vibration modes of T–O bonds, respectively (Bekkum *et al.*, 2001). The

Table 1. Chemical compositions (wt.%) of natural zeolite and the MZC.

Compound	SiO_2	Al_2O_3	Na_2O	TiO_2	K_2O	CaO	MgO	SrO	Fe_2O_3	LOI[a]	Total	Si/Al	TCEC[c]	CEC[c]
Zeolite	67.41	11.82	2.258	0.201	2.143	1.812	0.912	0.128	0.623	12.64	99.95	4.848	1.736	1.561
MZC	53.21	9.280	1.922	0.096	1.482	1.249	0.705	n.d.[b]	19.86	12.01	99.81	4.874	1.335	1.218

[a] Loss on ignition
[b] Not detected
[c] (meq g^{-1})

https://doi.org/10.1346/CCMN.2013.0610303 Published online by Cambridge University Press

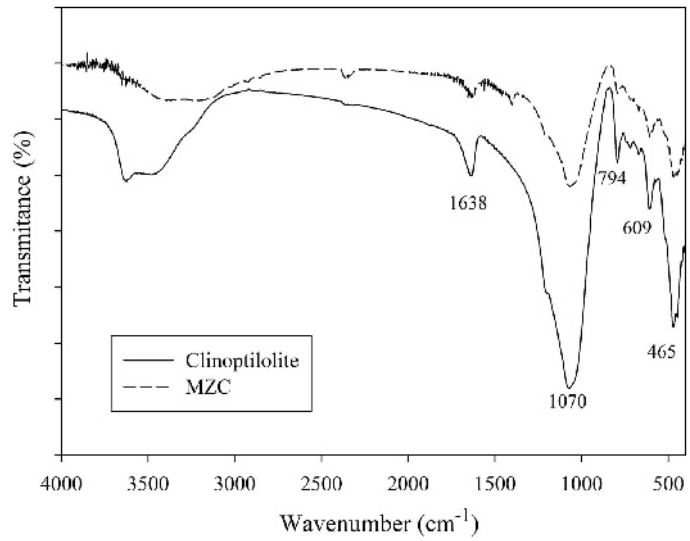

Figure 2. FTIR spectra of clinoptilolite and MZC.

characteristic band related to the Fe−O−Fe bond of Fe oxide must appear at 584 cm^{-1}, but this band was overlapped by the bands assigned to the double-ring stretching mode of zeolite (Maity and Agrawal, 2007).

In the DTG curves of the natural zeolite and composite, two weight-loss peaks were observed at temperatures below 100ºC (Figure 3). These dehydration peaks are attributed to the evaporation of water molecules which are located in different positions in the zeolite structure. At temperatures above 200ºC and up to 800ºC, the samples exhibited no weight-loss peaks, indicating that the samples were thermally stable.

Magnetic properties of the composite

The magnetic curve of the composite with 20% Fe oxide at 298 K (Figure 4) exhibited no hysteresis loop and no remanence which would indicate that the composite had satisfactory superparamagnetic properties. Consequently, the composite did not remain magnetized after exposure to an external magnetic field, and can be redispersed when the magnetic field is removed. The composite confirmed a saturation magnetization of ~17.46 Am^2/kg at 298 K, indicating sufficiently good magnetic property to be attracted by a permanent magnet. Because of the desirable magnetic properties and adsorption capacity, the composite with 20% Fe oxide was selected for adsorption experiments.

Effect of experimental condition on the adsorption process

Effect of pH. The evaluation of the pH effect (Figure 5) indicated that an acidic medium has an inhibitory effect on the uptake process. The lower uptake in acidic media was attributed to the competition by hydronium ions

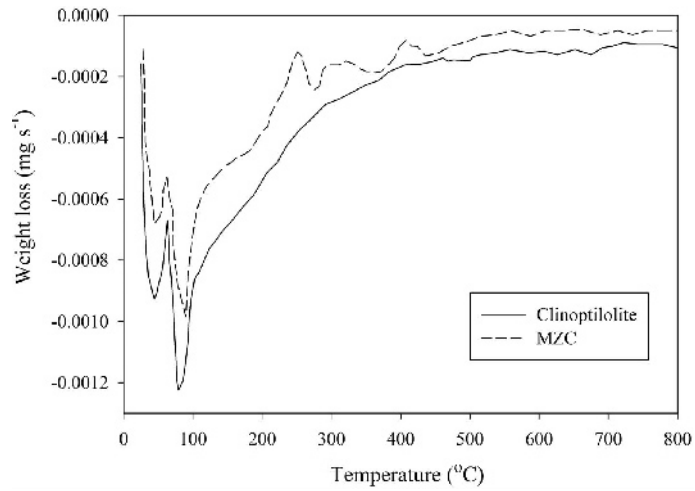

Figure 3. DTG curves of clinoptilolite and MZC.

https://doi.org/10.1346/CCMN.2013.0610303 Published online by Cambridge University Press

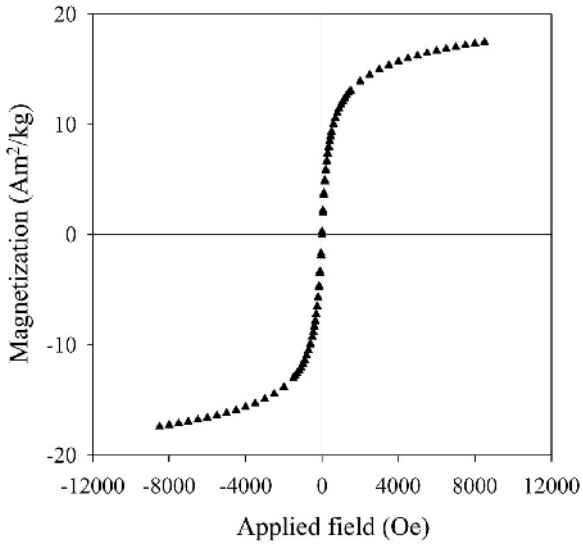

Figure 4. The hysteresis loops of MZC.

with Cs^+ and Sr^{2+} for the exchange sites. In addition, Fe oxide, as a weak acid or a weak base, participated in the cation exchange process according to the following reaction:

$$\text{Fe oxide}-\text{OH} + M^+ \rightarrow \text{Fe oxide}-\text{O}-M + \text{H}^+ \qquad (3)$$

Therefore, the total exchange capacity of the composite consisted of the exchangeability of both the zeolite and Fe oxide.

The concentration of deprotonated surface sites of Fe oxide increased with increasing pH value; therefore, the adsorption capacity of the composite increased with increasing pH and the maximal adsorption was observed at pH 8. In the present study, the pH was adjusted to 8.

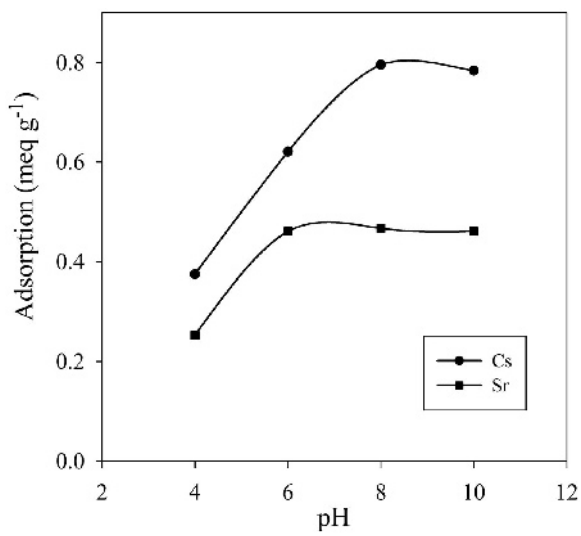

Figure 5. Effect of pH on sorption of Cs^+ and Sr^{2+}.

Effect of contact time. The effect of contact time on the cation adsorption capacity of the composite (Figure 6) was studied. The slope of the curves indicated that the adsorption rate was fast at the outset, but this initial rapid sorption subsequently gave way to a slow approach until equilibrium and saturation were reached after ~24 h. Based on the results collected, 24 h was taken as the equilibrium time in adsorption experiments.

Effect of temperature. The effect of adsorption temperature on removal of Cs^+ and Sr^{2+} (Figure 7) was studied over the temperature range 298–343 K. The adsorption capacity increased with increasing temperature, proving that the sorption process was endothermic. An increase in temperature caused progressive weakening of the ion-dipole forces between the cations and the solvent dipoles (water molecules), reducing the kinetic diameter of the ingoing ions. Therefore, greater numbers of hidden exchange sites within the zeolite framework participated in the sorption process. The data were used to estimate the thermodynamic variables.

Evaluation of thermodynamic variables

In order to identify the thermodynamic nature of the adsorption process, the value of enthalpy change (ΔH^o) and entropy change (ΔS^o) (Table 2) was calculated from the slopes and the intercepts of the linear plot of the Van't Hoff equation (Figure 8).

$$\ln k_d = -(\Delta H^o/RT) + (\Delta S^o/R) \qquad (4)$$

where k_d is the distribution coefficient, R is the universal gas constant (8.314 J mol^{-1} K^{-1}), and T is the absolute temperature (K). The change in Gibbs free energy of the adsorption (ΔG^o) was then calculated from:

$$\Delta G^o = \Delta H^o - T\Delta S^o \qquad (5)$$

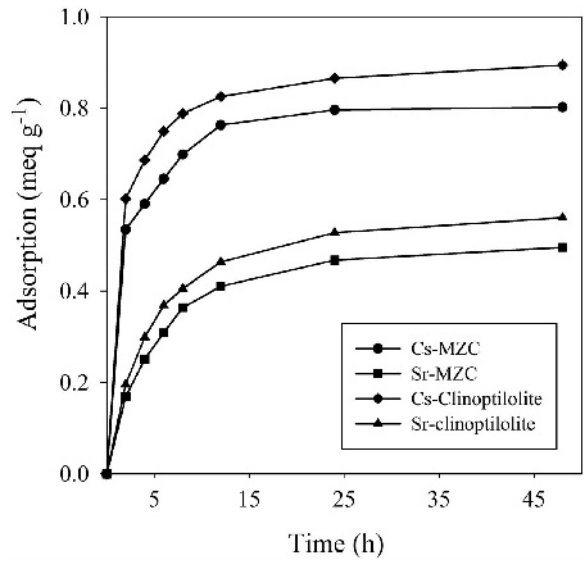

Figure 6. Effect of contact time on adsorption of Cs^+ and Sr^{2+} onto clinoptilolite and MZC.

https://doi.org/10.1346/CCMN.2013.0610303 Published online by Cambridge University Press

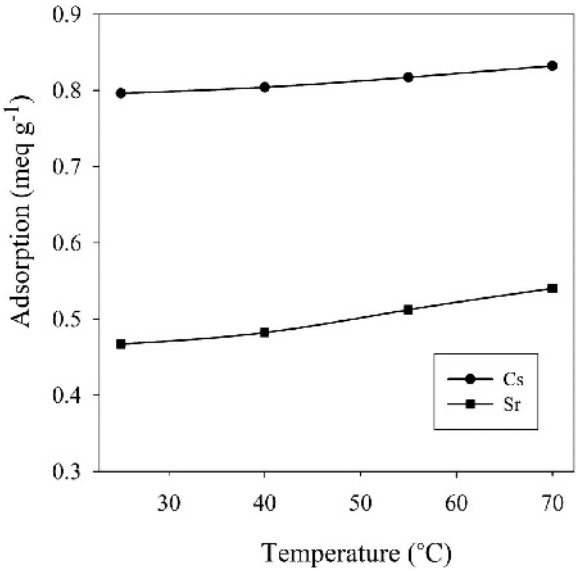

Figure 7. Effect of temperature on Cs^+ and Sr^{2+} adsorption.

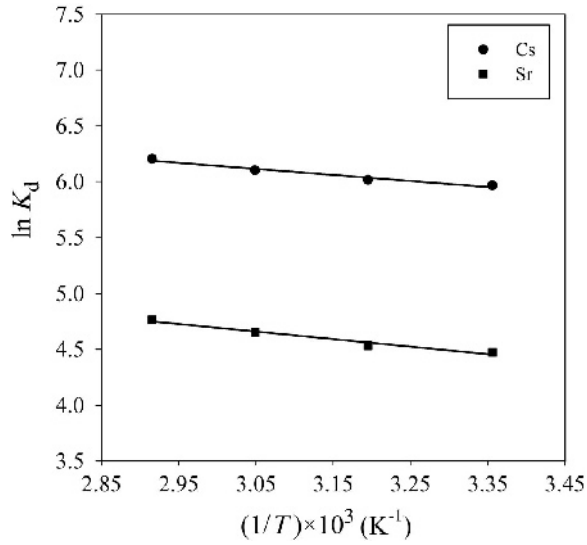

Figure 8. Van't Hoff plot for adsorption of Cs^+ and Sr^{2+}.

The adsorption process was endothermic because the ΔH^o values were positive. The positive values of ΔS^o showed that the randomness of the system was increased during the sorption process. The ΔG^o values were negative, indicating that an adsorption process occurred spontaneously. Also, for both ions, ΔG^o became more negative with increasing temperature, suggesting the favorable nature of sorption at higher temperature. Similar results have been found for Sr and Ba removal by dolomite (Ghaemi *et al.*, 2011) and Zr removal by clinoptilolite (Faghihian and Kabiri-Tadi, 2010). Greater absolute values of ΔG^o for Cs^+ indicated that its adsorption is more favored than that of Sr^{2+}.

Kinetics study

Both pseudo-first order and pseudo-second order kinetics models were used to estimate the kinetics parameters. The conformity between experimental data and kinetics models was expressed by the correlation coefficients (R). Also, the values of calculated q_e were compared with the experimental data.

The linear forms of the pseudo-first order model of Lagergren and pseudo-second order model are, respectively:

$$\ln (q_e - q_t) = \ln q_e - k_1 t \quad (6)$$

$$t/q_t = 1/(k_2 q_e^2) + (1/q_e)t \quad (7)$$

and the initial sorption rate, h (mmol g^{-1} min^{-1}), was obtained from:

$$h = k_2 q_e^2 \quad (8)$$

where q_e and q_t are the amount of ions adsorbed per unit mass of composite at equilibrium and at any time, t (mmol g^{-1}), respectively. k_1 and k_2 are the rate constants of the pseudo-first order (min^{-1}) and pseudo-second order (g mg^{-1} min^{-1}) models (Table 3). The value of the correlation coefficients (R^2) and agreement of calculated q_e with experimental data indicated that the sorption process can be described well by the pseudo-second order equation. Therefore, the overall rate constant of both sorption processes appears to be controlled by chemical sorption (McKay and Ho, 1999; Karadag *et al.*, 2007).

For comparison, experimental data from natural clinoptilolite were also fitted to pseudo-first and -second order models (Table 3). The rate constant for the composite was greater than that for zeolite, which was attributed to the nanosize and large surface area of the magnetite on the surface of zeolite contributing to

Table 2. Thermodynamic variables calculated for the sorption of Cs^+ and Sr^{2+} onto MZC.

Ion	E_a (kJ mol^{-1})	ΔH^o (kJ mol^{-1})	ΔS^o (kJ mol^{-1})	ΔG^o (kJ mol^{-1}) 298K	313K	328K	343K
Cs^+	3.633	4.496	0.0645	−14.725	−15.692	−16.660	−17.627
Sr^{2+}	4.319	5.616	0.0559	−11.042	−11.880	−12.719	−13.558

https://doi.org/10.1346/CCMN.2013.0610303 Published online by Cambridge University Press

Table 3. Kinetics of Cs^+ and Sr^{2+} adsorption onto MZC.

Sorbent	Ion	$q_{e(exp.)}$ ($\times 10^{-1}$) (mmol g^{-1})	pseudo-first order model				pseudo-second order model			
			k_1 ($\times 10^{-2}$) (min^{-1})	$q_{e(theor.)}$ ($\times 10^{-1}$) (mmol g^{-1})	R^2	k_2 ($\times 10^{-1}$) (g $mmol^{-1}$ min^{-1})	q_e ($\times 10^{-1}$) (mmol g^{-1})	h ($\times 10^{-2}$) (mmol g^{-1} min^{-1})	R^2
Zeolite	Cs^+	8.940	0.169	2.867	0.9534	0.1418	9.163	1.1902	0.9999
	Sr^{2+}	2.800	0.177	1.942	0.9856	0.1373	3.043	0.1272	0.9999
MZC	Cs^+	8.020	0.297	4.092	0.9930	0.1497	8.277	1.0256	0.9996
	Sr^{2+}	2.470	0.186	1.809	0.9864	0.1453	2.702	0.1069	0.9995

sorption process. The k_2 values were selected for evaluation of E_a using the Arrhenius equation (Figure 9).

$$\ln k_2 = \ln A - E_a/RT \quad (9)$$

where k_2 and A are the rate constant and temperature independent factor (g $mmol^{-1}$ min^{-1}), respectively; E_a is the activation energy of the sorption (J mol^{-1}). The values of E_a were calculated from the slope of ln k_2 *vs.* $1/T$ (Table 2). The values of E_a were <42.0 J mol^{-1}, suggesting that adsorption of Cs^+ and Sr^{2+} proceeded with a low potential energy (Scheckel and Sparks, 2001).

Sorption isotherm study

The effect of ion concentrations on the uptake behavior of the magnetic composite was investigated in the concentration range 0.001–0.1 meq mL^{-1}. The relationship between the amount of ions adsorbed per unit mass of the composite, and the concentration of the ions remaining in solution at equilibrium represented the sorption isotherm (Figure 10a,b). Three isotherm models (Langmuir, Freundlich, and D-R) were used to evaluate the experimental data.

Langmuir isotherm model

The Langmuir isotherm assumes that the sorption occurs at specific homogeneous sites within the adsorbent. The linearized form of this model is given by:

$$C_e/q_e = 1/(Q_0 b) + C_e/Q_0 \quad (10)$$

where Q_0 is the monolayer saturation adsorption capacity (mg g^{-1}) and b is the constant related to the enthalpy of adsorption, which were calculated from the slope and the intercept of equation 10 (Figure 11). The Langmuir model can be used to estimate the maximum adsorption capacity corresponding to complete monolayer coverage of the adsorbent. The values of Q_0

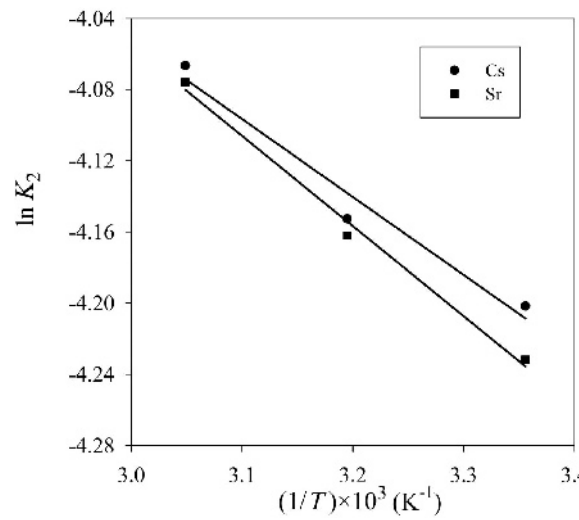

Figure 9. Arrhenius plot for adsorption of Cs^+ and Sr^{2+}.

https://doi.org/10.1346/CCMN.2013.0610303 Published online by Cambridge University Press

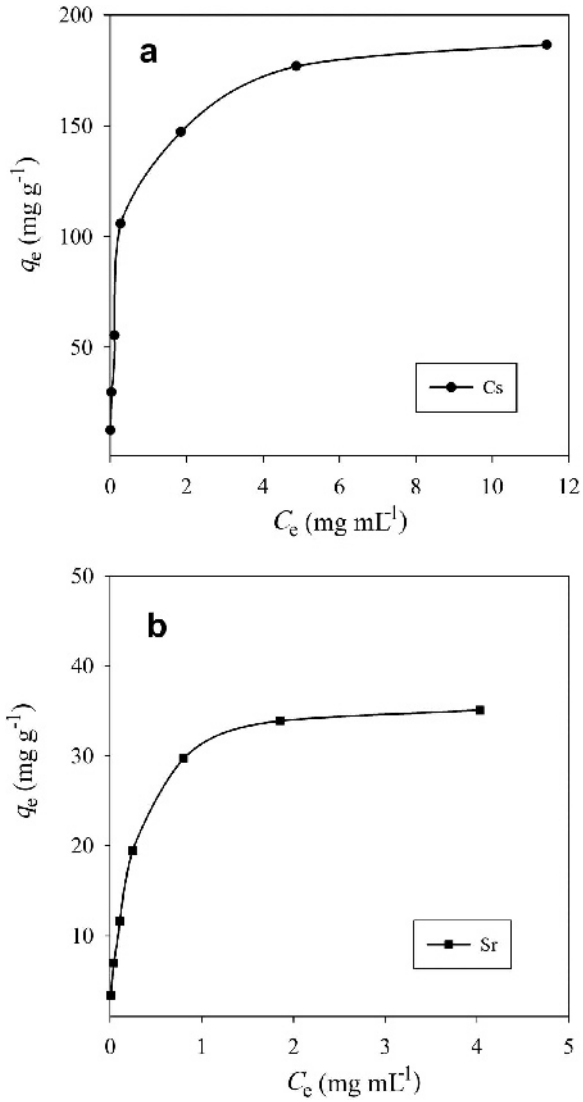

Figure 10. Effect of different initial ion concentrations on sorption of Cs^+ (a) or Sr^{2+} (b).

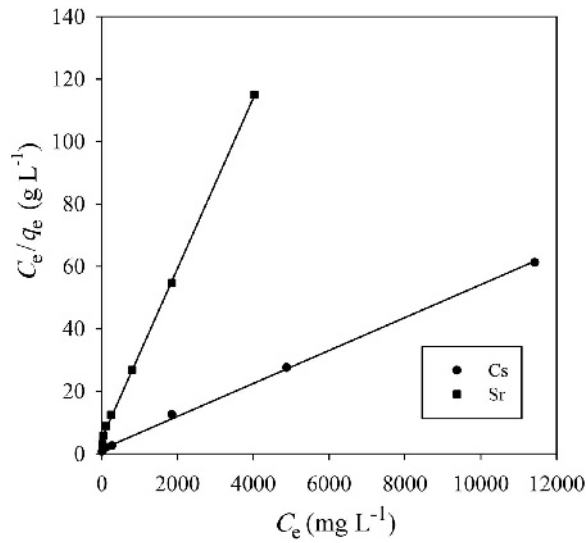

Figure 11. Langmuir isotherm plots for adsorption of Cs^+ and Sr^{2+}.

confirmed the large adsorption capacity of the composite prepared for Cs^+ and Sr^{2+} (Table 4).

The important parameter of the Langmuir isotherm model is the dimensionless constant, R_L, which could be calculated from:

$$R_L = 1/(1 + bC_0) \quad (11)$$

where C_0 is the largest initial ion concentration (mg L^{-1}). The value of R_L gives an indication of whether the process is unfavorable ($R_L > 1$), linear ($R_L = 1$), favorable ($0 < R_L < 1$), or irreversible ($R_L = 0$) (Mohan and Chander, 2006). The data obtained confirmed that adsorption was favorable for Cs^+ and Sr^{2+}.

The maximum adsorption capacities of MZC for the removal of Cs^+ and Sr^{2+} were compared with those of some natural adsorbents reported in the literature (Table 5). The MZC exhibited significant adsorption capacity for these ions. Most importantly, the separation of the magnetic composite from solution was easily achieved using a permanent magnet.

Table 4. Adsorption isotherm parameters for Cs^+ and Sr^{2+} adsorption onto MZC.

		Model parameters			
Isotherm	Ion	q_0 (mg g^{-1})	b × 10^3 (L mg^{-1})	$R_L \times 10^3$	R^2
Langmuir	Cs^+	188.7	3.759	19.62	0.9991
	Sr^+	36.63	5.716	38.40	0.9992
		n	K_f (mg g^{-1})	R^2	
Freundlich	Cs^+	2.705	8.147	0.916	
	Sr^+	2.455	1.604	0.9492	
		β × 10^{-9} (mol^2 kJ^{-2})	q_m (mmol g^{-1})	E (kJ mol^{-1})	R^2
D-R	Cs^+	5.174	1.992	9.831	0.9799
	Sr^{2+}	6.321	1.144	8.894	0.9913

https://doi.org/10.1346/CCMN.2013.0610303 Published online by Cambridge University Press

Table 5. Adsorption capacity, q_m, of Cs^+ and Sr^{2+} by various adsorbents.

Adsorbent	q_m (mg g^{-1})		Reference
	Cs^+	Sr^{2+}	
Natural clinoptilolite	132.9	–	(Borai *et al.*, 2009)
Montmorillonite	57.04	13.26	(Ma *et al.*, 2011)
Phosphate-modified montmorillonite	93.87	12.56	(Ma *et al.*, 2011)
Taiwan laterite	39.87	–	(Wang *et al.*, 2008)
Dolomite	–	1.172	(Ghaemi *et al.*, 2011)
Natural zeolite	205.8	41.36	Present study
Magnetic zeolite composite	188.7	36.63	Present study

Freundlich isotherm model

The Freundlich isotherm model assumes that sorption occurs at heterogeneous surfaces on which the adsorption energy changes exponentially with surface coverage. This model was used to estimate the intensity of the adsorption process and relative sorption capacity. The linearized form of the Freundlich model is written as

$$\log q_e = \log K_f + 1/n \log C_e \quad (12)$$

where K_f is the Freundlich constant related to the adsorbent capacity, and n is a constant, indicative of the intensity of the absorption process. The values of the constants n and K_f were calculated from the slope and the intercept of equation 12 (Figure 12). The value of n was >1, illustrating that significant adsorption had taken place even at high ion concentrations. The value for K_f for MZC was greater for Cs^+ than for Sr^{2+}, indicating that the composite had a greater affinity for Cs^+ (Table 4).

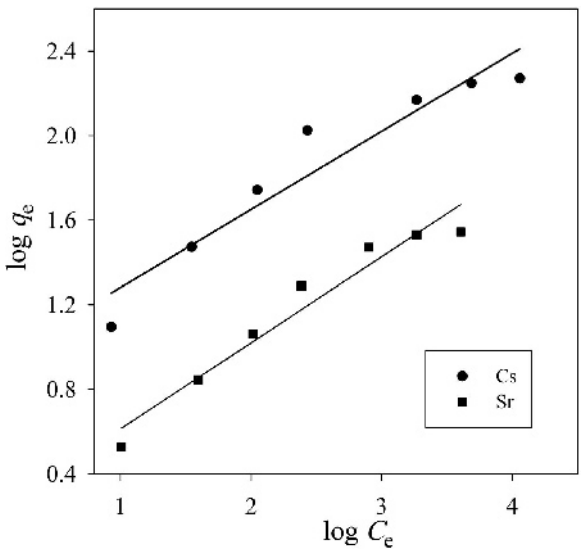

Figure 12. Freundlich isotherm plots for adsorption of Cs^+ and Sr^{2+}.

D-R isotherm model

The D-R isotherm model distinguishes between the physical and chemical nature of the sorption process. This equation is given as follows:

$$\ln q_e = \ln q_m - \beta\varepsilon^2 \quad (13)$$

where q_m is the maximum adsorption capacity (meq g^{-1}), β is the constant related to the adsorption energy (mol^2 kJ^{-2}), and ε is the Polanyi potential:

$$\varepsilon = RT \ln (1 + 1/C_e) \quad (14)$$

where R is the gas constant (8.314 kJ mol^{-1} K^{-1}) and T is absolute temperature (K). The experimental data were fitted to this isotherm model (Figure 13). The mean internal energy of adsorption, E (kJ mol^{-1}), is defined as the change in internal energy when 1 mole of ions is transferred to the surface of the composite from infinity of the solution, and is calculated from:

$$E = (2\beta)^{-1/2} \quad (15)$$

The E value in the range 8–16 kJ mol^{-1} indicates that the sorption process is achieved *via* exchange.

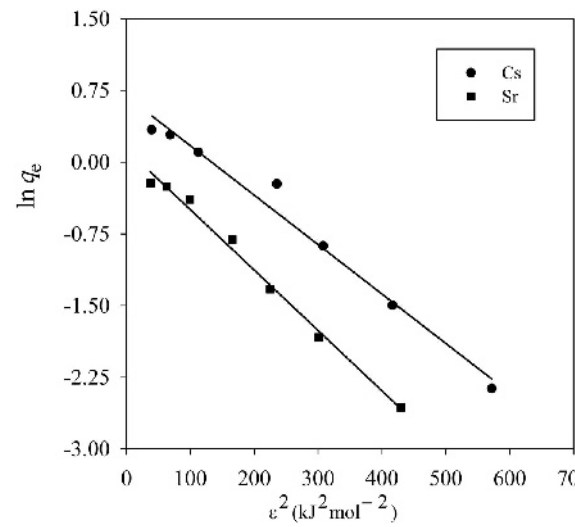

Figure 13. D-R isotherm plots for adsorption of Cs^+ and Sr^{2+}.

https://doi.org/10.1346/CCMN.2013.0610303 Published online by Cambridge University Press

Physical force is involved in the sorption process if E<8 kJ mol^{-1} (Helfferich, 1962). The E values obtained for adsorption of Cs^+ and Sr^{2+} were in the range 8−16 kJ mol^{-1}, indicating that both ions were taken up *via* an ion-exchange, or chemical adsorption, process (Table 4).

CONCLUSIONS

In the present study, a natural zeolite nanomagnetite composite was synthesized, characterized, and evaluated for removal of Cs^+ and Sr^{2+} from aqueous solutions. The crystal structure of zeolite was not changed during the magnetic modification. The VSM results confirmed that the composite was sufficiently magnetic to be attracted by a magnetic field. A pseudo-second order model gave better correlation with the experimental kinetics data than pseudo-first order, confirming that chemical sorption was the dominant process. The rate-constant values for sorption by MZC were greater than the values obtained for natural zeolite, indicating a faster rate of adsorption by the composite. The negative ΔG^o value and positive ΔH^o value indicated that the adsorption of both ions was spontaneous and endothermic. The R_L values obtained were in the range 0−1, indicating that adsorption of Cs^+ and Sr^{2+} were favored. The composite demonstrated large CEC capacity and fast adsorption kinetics for Cs^+ and Sr^{2+}, as well as good magnetic behavior, making it easy to separate from the aqueous solution.

ACKNOWLEDGMENTS

Financial support of this work by the Center of Excellence of Chemistry and Research Council of the University of Isfahan is gratefully appreciated.

REFERENCES

Abdel Rahman, R.O., Ibrahim, H.A., Hanafy, M., and Abdel Monem, N.M. (2010) Assessment of synthetic zeolite Na A−X as sorbing barrier for strontium in a radioactive disposal facility. *Chemical Engineering Journal*, **157**, 100−112.

Archibald, R.M. and Seligson, D. (1957) *Standard Methods of Clinical Chemistry*. Academic Press, New York.

Ashtari, P., Wang, K., Yang, X., Huang, S., and Yamini, Y. (2005) Novel separation and preconcentration of trace amounts of copper (II) in water samples based on neocuproine modified magnetic microparticles. *Analytica Chimica Acta*, **550**, 18−23.

Bachir, C., Lan, Y., Mereacre, V., Powell, A.K., Bender Koch, C., and Weidler, P.G. (2009) Magnetic titanium-pillared clay (Ti-M-PILC): Magnetic studies and Mössbauer spectroscopy. *Clays and Clay Minerals*, **57**, 433−443.

Balarama Krishna, M.V., Rao, S.V., Arunachalam, J., Murali, M.S., Kumar, S., and Manchanda, V.K. (2004) Removal of ^{137}Cs and ^{90}Sr from actual low level radioactive waste solutions using moss as a phyto-sorbent. *Separation and Purification Technology*, **38**, 149−161.

Bekkum, H.V., Flanigen, E.M., and Janson, J.C. (2001) *Introduction to Zeolite Science and Practice*. Elsevier, Amsterdam.

Borai, E.H., Harjula, R., Malinen, L., and Paajanen, A. (2009) Efficient removal of cesium from low-level radioactive liquid waste using natural and impregnated zeolite minerals. *Journal of Hazardous Materials*, **172**, 416−422.

Bourlinos, A.B., Zboril, R., and Petridis, D. (2003) A simple route towards magnetically modified zeolites. *Microporous and Mesoporous Materials*, **58**, 155−162.

Breck, D.W. (1974) *Zeolite Molecular Sieves, Structure, Chemistry and Uses.* Wiley, New York.

El-Naggar, M.R., El-Kamash, A.M., El-Dessouky, M.I., and Ghonaim, A.K. (2008) Two-step method for preparation of NaA-X zeolite blend from fly ash for removal of cesium ions. *Journal of Hazardous Materials*, **154**, 963−972.

Faghihian, H. and Kabiri-Tadi, M. (2010) Removal of zirconium from aqueous solution by modified clinoptilolite. *Journal of Hazardous Materials*, **178**, 66−73.

Ghaemi, A., Torab-Mostaedi, M., and Ghannadi-Maragheh, M. (2011) Characterizations of strontium(II) and barium(II) adsorption from aqueous solutions using dolomite powder. *Journal of Hazardous Materials*, **190**, 916−921.

Gutierrez, M., Escudey, M., Escrig, J., Denardin, J., Altbir, D., Fabris, J., Cavalcante, L., and García-González, M.T. (2010) Preparation and characterization of magnetic composites based on a natural zeolite. *Clays and Clay Minerals*, **58**, 585−595.

Helfferich, F. (1962) *Ion exchange.* McGraw Hill, New York.

Kabiri-Tadi, M. and Faghihian, H. (2011) Removal of ruthenium from aqueous solution by clinoptilolite. *Clays and Clay Minerals*, **59**, 34−41.

Karadag, D., Koc, Y., Turan, M., and Ozturk, M. (2007) A comparative study of linear and non-linear regression analysis for ammonium exchange by clinoptilolite zeolite. *Journal of Hazardous Materials*, **144**, 432−437.

Klug, H.P. and Alexander, L.E. (1974) *X-ray Diffraction Procedures: for Polycrystalline and Amorphous Materials.* John Wiley & Sons, New York.

Ma, B., Oh, S., Shin, W.S., and Choi, S.J. (2011) Removal of Co^{2+}, Sr^{2+} and Cs^+ from aqueous solution by phosphate-modified montmorillonite (PMM). *Desalination*, **276**, 336−346.

Maity, D. and Agrawal, D.C. (2007) Synthesis of iron oxide nanoparticles under oxidizing environment and their stabilization in aqueous and non-aqueous media. *Journal of Magnetism and Magnetic Materials*, **308**, 46−55.

McKay, G. and Ho, Y.S. (1999) Pseudo-second order model for sorption processes. *Process Biochemistry*, **34**, 451−460.

Mohan, D. and Chander, S. (2006) Single, binary and multi-component sorption of iron and manganese on lignite. *Journal of Colloid and Interface Science*, **299**, 57−76.

Nah, I.W., Hwang, K.Y., Jeon, C., and Choi, H.B. (2006) Removal of Pb ion from water by magnetically modified zeolite. *Minerals Engineering*, **19**, 1452−1455.

Oliveira, L.C.A., Petkowicz, D.I., Smaninotto, A., and Pergher, S.B.C. (2004) Magnetic zeolites: a new adsorbent for removal of metallic contaminants from water. *Water Research*, **38**, 3699−3704.

Shakir, K., Sohsah M., and Soliman, M. (2007) Removal of cesium from aqueous solutions and radioactive waste simulants by coprecipitate flotation. *Separation and Purification Technology*, **54**, 373−381.

Scheckel, K.G. and Sparks, D.L. (2001) Temperature effects on nickel sorption kinetics at mineral water interface. *Soil Science Society of America Journal*, **65**, 719−728.

Treacy, M.M.J. and Higgins, J.B. (2007) *Collection of Simulated XRD Powder Patterns for Zeolites.* Elsevier, Amsterdam.

Wang, T.H., Li, M.H., Yeh, W.C., Wei, Y.Y., and Teng, S.P. (2008) Removal of cesium ions from aqueous solution by adsorption onto local Taiwan laterite. *Journal of Hazardous*

Materials, **160**, 638–642.
Wu, P., Daia, Y., Long, H., Zhu, N., Li, P., Wu, J., and Dang, Z. (2012) Characterization of organo-montmorillonites and comparison for Sr(II) removal: equilibrium and kinetic studies. *Chemical Engineering Journal*, **191**, 288–296.
Zhang, C., Gu, P., Zhao, J., Zhang, D., and Deng, Y. (2009) Research on the treatment of liquid waste containing cesium by an adsorption–microfiltration process with potassium zinc hexacyanoferrate. *Journal of Hazardous Materials*, **167**, 1057–1062.

(*Received 6 December 2012; revised 26 March 2013; Ms. 733; AE: S.M. Kuznicki*)